THE JOURNAL OF PHYSICAL CHEMISTRY C

Article

Cite This: J. Phys. Chem. C 2017, 121, 25882-25887

pubs.acs.org/JPCC

Highly Efficient Regeneration of Deactivated Au/C Catalyst for 4-Nitrophenol Reduction

Mingbo Ruan,[†] Ping Song,[†] Jing Liu,[†,‡] Erling Li,[†,‡] and Weilin Xu*[,†]

[†]State Key Laboratory of Electroanalytical Chemistry, Changchun Institute of Applied Chemistry, Jilin Province Key Laboratory of Low Carbon Chemical Power, Chinese Academy of Science, 5625 Renmin Street, Changchun 130022, P. R. China

[‡]Graduate University of Chinese Academy of Science, Beijing, 100049, China

Supporting Information

ABSTRACT: In the present work, we proposed an effective method to regenerate sintered gold catalyst by improving the dispersion of gold nanoparticles. With the liquid oxychlorination reaction, a sintered carbon-supported gold (Au/C) nanocatalyst was effectively regenerated by improving the redispersion of Au nanoparticles with additional carbon support. The Au-catalyzed model reaction between 4-nitrophenol and sodium borohydride ($NaBH_4$) indicates that the apparent activity of the optimal Au/C regenerated (Au 0.45 wt %) exceeds that of the initial fresh Au/C (Au 1 wt %), making Au utilization tripled and potentially sustainable for their extensive application in industry.

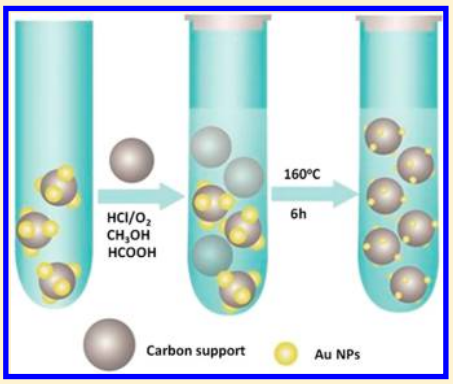

1. INTRODUCTION

Over the past decades, gold-based catalysts have been investigated broadly due to their extensive application in all kinds of heterogeneous reactions,[1−3] such as CO oxidation,[4] and hydroaminations.[5,6] These catalysts have many advantages in application; however, it is well-known that deactivation of these catalysts is an unavoidable problem, mainly due to their physical or chemical variations. The variations occur via different mechanisms, such as sintering, coking, and poisoning or agglomeration of metal nanoparticles.[7,8] Due to the rarity of gold on earth, it is very desirable for us to regenerate gold catalysts by improving the redispersion of gold nanoparticles.[9−11] The sintering-induced inactivation of catalysts can be reversed or regenerated by redispersing the sintered metal nanoparticles on the support.[12] The complicated metal redistribution on the support is physically and chemically dependent on experimental conditions, such as time, temperature, metal loading, support, atmosphere, etc. Redispersion of metals has been applied successfully for the regeneration of many different metal catalysts (Pt, Pd, Rh, Co, Ni, Ag, etc.).[13] Recently, some attention had been paid to the regeneration of supported gold nanoparticles by improving their redispersion with different approaches.[14−17] All of these regenerations were based on the simple redispersion of the same or even lesser amount of metals on the same amounts of supports.[13] Obviously, to some extent, such simple redispersion of metals can regenerate the catalytic activity of sintered catalysts to some extent, but not that much for practical applications of noble metals. Recently, on the basis of additional carbon support only, we proposed a simple method to regenerate the activity of sintered catalysts with the mass and Pt utilization doubled of carbon-supported Pt catalysts.[18,19]

Herein, with additional carbon support, we present an improved protocol by replacing gas CH_3Cl with diluted chloride acid (5% HCl) to regenerate the sintered catalysts with the mass doubled of carbon-supported gold (Au/C) (Scheme 1).[14−17] In this way, the redispersion of Au metal can be improved tremendously by the surface of additional carbon support. For the catalytic reaction between 4-nitrophenol and sodium borohydride ($NaBH_4$), the metal (Au) utilization of the optimal regenerated Au/C (Au 0.45 wt %) is more than 3 times (320%) of the original fresh Au catalyst (Au/C, with Au 1 wt %). With such a technique, in principle, one can acquire sustainable application of all kinds of noble metals.

2. EXPERIMENTAL SECTION

2.1. Materials. Vulcan XC-72 carbon black was from E-TEK Co. Carbon support (Black Pearls, BP2000) was from Asian-Pacific Specialty Chemicals. 4-Nitrophenol, sodium borohydride ($NaBH_4$), methanol (CH_3OH), formic acid (HCOOH), hydrochloric acid (HCl), and tetrachloroauric acid tetrahydrate ($HAuCl_4{\cdot}4H_2O$) salt were from Sigma-Aldrich. Ultrapure water (18.23 MΩ·cm in resistance) was from ion exchange and filtration after reversed osmosis. High-purity N_2 (99.99%) was purchased from Changchun Gas Co., China.

Received: September 4, 2017
Revised: October 25, 2017
Published: November 9, 2017

DOI: 10.1021/acs.jpcc.7b08787
J. Phys. Chem. C 2017, 121, 25882−25887

Scheme 1. Regeneration Mechanism of Metal Catalysts with Additional Pure Support

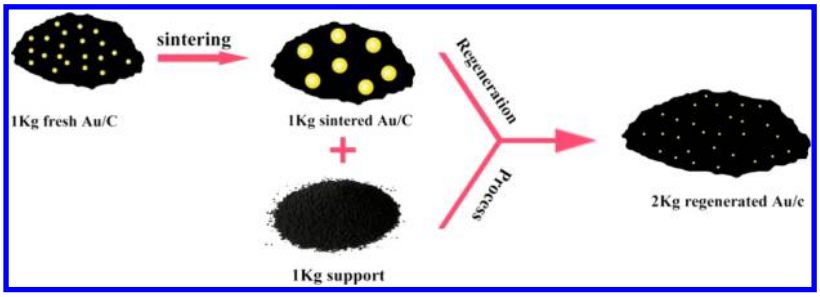

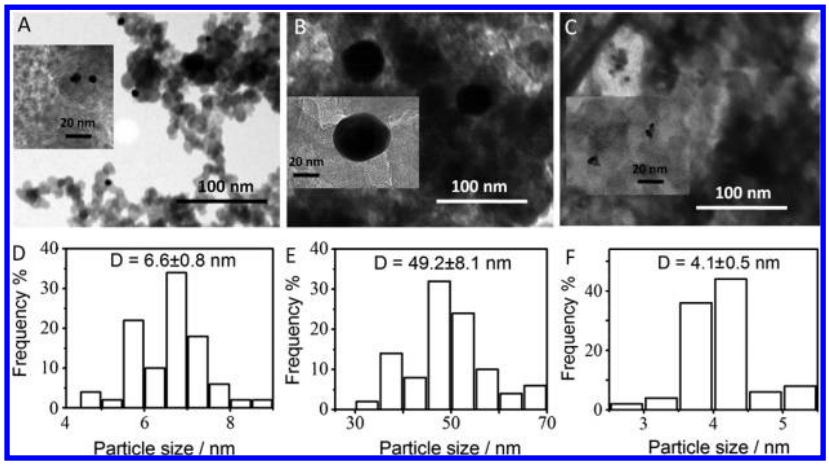

Figure 1. TEM characterization and size distributions of Au/C catalysts: (A, D) fresh Au/C (Au-F), (B, E) sintered Au/C (Au-S), and (C, F) Au/C obtained (Au-R) after the reforming or regeneration of Au-S.

2.2. Synthesis of Fresh Au/C Catalyst and the Sintering. The synthesis and sintering method is based on our previous work.[18] Vulcan XC-72 is the carbon support and $HAuCl_4$ is the gold precursor. The support of Vulcan XC-72 (1.0 g) was dispersed homogeneously in 100 mL of deionized water with a certain amount of Au precursor by sonication of 30 min. Then, $NaBH_4$ solution was dropped slowly to reduce the Au precursor under vigorous stirring. The obtained precipitate was filtered and washed with deionized water, and finally dried at 120 °C overnight to give Au/C. ICP was used to determine the Au content (about 1 wt %) on fresh Au/C (labeled as Au-F). The Au-F was heated in a N_2 atmosphere at 900 °C for 3 h to obtain sintered catalyst (labeled as Au-S with Au 1.1 wt %).

2.3. Regeneration of Sintered Au/C. It was found here that O_2/HCl can dissolve Au nanoparticles into $AuCl_4^-$, and the $AuCl_4^-$ can be reduced back into Au^0 by formic acid at 160 °C. On the basis of these two reversible processes, a regeneration or redispersion reaction system containing O_2, HCl, formic acid, and Au/C was designed with a sealed glass reactor from SynthWare as shown in Figure S1 (Supporting Information).

2.4. Reduction of 4-Nitrophenol in the Presence of Au/C Catalysts. The catalytic reaction between 4-nitrophenol and $NaBH_4$ was carried out in a 20 mL glass cuvette with 16 mL of solution in the presence of Au/C catalysts. While evaluating the quantification of the activity of catalysts, the final concentration of catalysts was kept at 10 μg/mL, 4-nitrophenol at 1.0×10^{-4} M, and $NaBH_4$ at 1×10^{-2} M. The reaction was spectrophometrically monitored at 400 nm at 5 min intervals.

2.5. Physical Characterization of Catalysts. The structures of the catalysts were characterized with transmission electron microscopy (TEM, JEM-2100F microscope) and the powder X-ray diffraction (XRD, Shimadzu XRD-6000 diffractometer with Cu K-alpha radiation) patterns. The Au contents in these catalysts were analyzed with ICP (ICAP-6000, Thermo Fisher Scientific). The activity of Au/C was evaluated by calculating the rates of reduction of 4-nitrophenol.

3. RESULTS AND DISCUSSION

As shown in Figure 1A, the Au nanoparticles on freshly obtained Au/C catalysts (Au-F with Au 1 wt %) possess an average diameter of 6.6 ± 0.8 nm. After the sintering of Au-F at 900 °C under N_2 flow, as expected, larger Au nanoparticles with an average size of 49.2 ± 8.1 nm were observed (labeled as Au-S, Figure 1B). The regeneration protocol of Au-S (Figure S1, Supporting Information) was based on our observation that the fresh colloid Au nanoparticles obtained from $HAuCl_4$ reduction could be redissolved into $AuCl_4^-$ when the colloid solution is boiled.

According to previous knowledge,[18,19] the redissolving of colloid Au nanoparticles into $AuCl_4^-$ was actually based on an oxychlorination process. By this process, it was finally realized that oxygen/hydrochloric acid (HCl) in a sealed atmosphere can dissolve Au nanoparticles into $AuCl_4^-$ (Figure S2, Supporting Information), which could be further reduced back to Au^0 by formic acid at 160 °C (Scheme 2). The freshly obtained Au^0 atoms will deposit either on the surface of carbon as nuclei for the growth of new Au nanoparticles or on the surface of existent Au nanoparticles. The above reversible process proceeds simultaneously for many cycles to reach a new equilibrium state (Scheme 2A) with the depletion of O_2/HCl and formic acid. In this way, the large Au nanoparticles will be redispersed or regenerated on the support with an improved

DOI: 10.1021/acs.jpcc.7b08787
J. Phys. Chem. C 2017, 121, 25882−25887

Scheme 2. Redispersion Mechanism of Au Nanoparticles on Additional Carbon Support

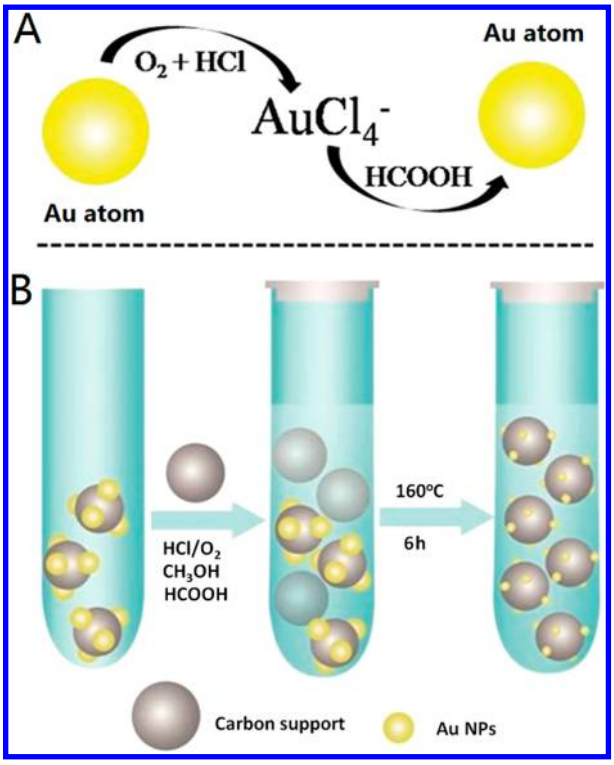

redispersion. The Au nanoparticles on optimal regenerated catalyst (labeled as Au-R) possess an average size of 4.1 ± 0.5 nm (Figure 1C).

In order to obtain a large-scale image of the catalysts, SEM was used to examine these catalysts at much lower magnification using back scattered electron imaging. As shown in Figure 2, compared with the fresh Au/C, the Au nanoparticles on sintered catalyst are much larger in size, while, after the regeneration process, the average size of Au nanoparticles decreased hugely and is even smaller than the fresh one, consistent with the TEM results shown in Figure 1.

For the further reduction of $AuCl_4^-$ by formic acid (Scheme 2A), a competition or balance exists between the dissolving and deposition of Au species. The improvement of Au redispersion on carbon was achieved by driving the balance to the right side with additional carbon support (Scheme 2B). The mechanism for such improvement is that the newly added carbon support supplements lots of new nucleation sites for newly formed Au^0 atoms.[18]

It should be noted here, for the purpose of obtaining the optimal regeneration condition, based on the optimal temperature of 160 °C and optimal amount (6 mg) of carbon support added for the regeneration of 6 mg of sintered Pt/C catalysts,[18,19] in this case, we further optimized the reaction time and the mass ratio between hydrochloric acid and formic

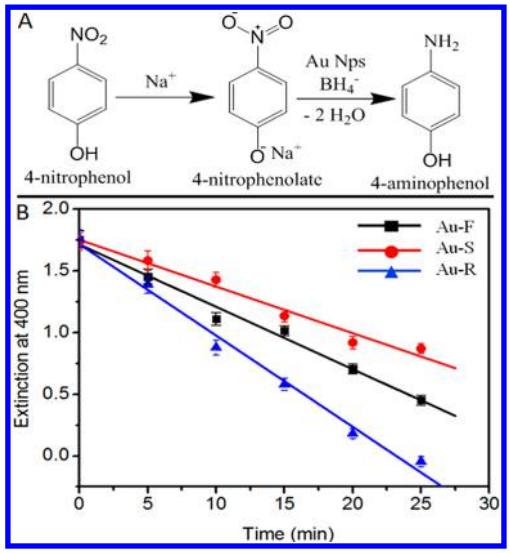

Figure 3. (A) The mechanism of the Au-catalyzed reduction reaction of 4-nitrophenol by $NaBH_4$. (B) Catalytic reaction rates of 4-nitrophenol reduction by $NaBH_4$ with three different (Au-F, Au-S, and Au-R) catalysts at the same loading of 1.6 $\mu g_{catalyst}$ mL^{-1} at 25 °C.

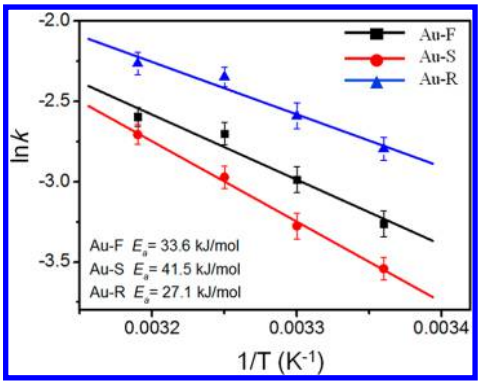

Figure 4. Plot of ln k versus $1/T$ for 4-nitrophenol reduction by $NaBH_4$ catalyzed by different catalysts.

Table 1. Au 4f XPS Data for Different Au/C Catalysts

	atomic ratio of Au species/%		
	Au^0	Au^+	Au^{3+}
Au-F	25.8	65.9	8.3
Au-S	79.2	20.8	
Au-R	24.6	75.4	

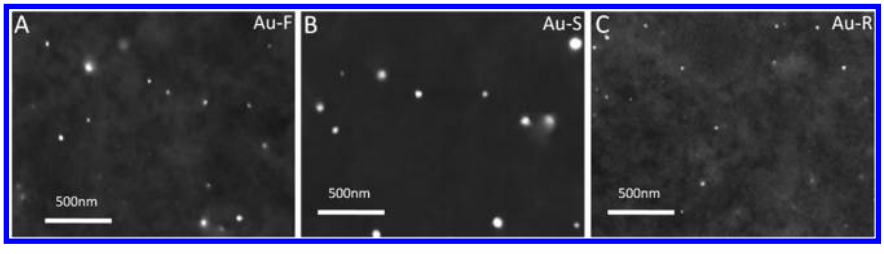

Figure 2. SEM characterization of different Au/C catalysts: (A) fresh Au/C (Au-F), (B) sintered Au/C (Au-S), (C) regenerated Au/C (Au-R) from Au-S.

DOI: 10.1021/acs.jpcc.7b08787
J. Phys. Chem. C 2017, 121, 25882−25887

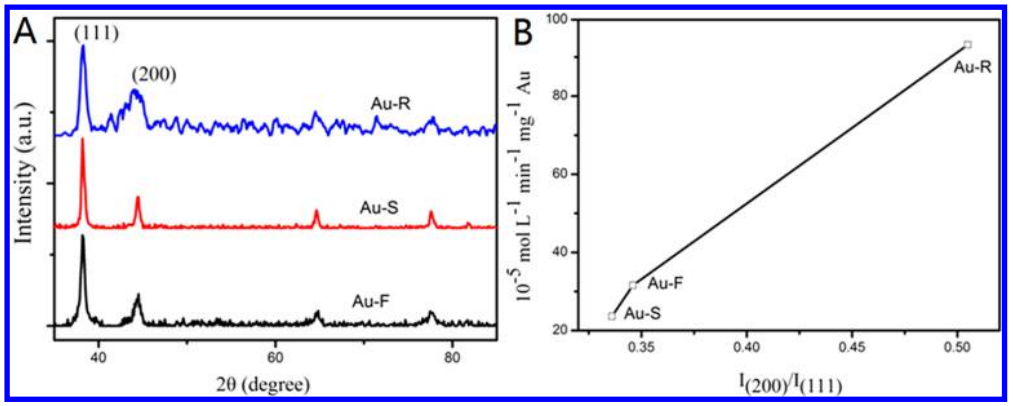

Figure 5. (A) XRD spectra of different Au/C catalysts. (B) Correlation between $I_{(200)}/I_{(111)}$ and Au utilization (10^{-5} M/min mg^{-1} Au) of different Au/C catalysts.

acid (Figures S4 and S5, Supporting Information) for the regeneration of sintered Au/C. Finally, on the basis of the following Au-catalyzed model reaction, we obtained the optimal regeneration of 6 mg of sintered Au/C (Au-S) catalyst at 160 °C with the ratio of hydrochloric acid and formic acid of 1 to 3 and a reaction time of 6 h. ICP results show the Au contents on sintered Au/C (Au-S) and optimal regenerated Au/C (Au-R) are about 1.1 and 0.45 wt %, respectively, indicating about 18.2% of Au remained in the solution in the form of $AuCl_4^-$.

In order to evaluate quantitatively the activity of regenerated catalysts, a Au-catalyzed model reduction reaction from 4-nitrophenol (or more accurately, 4-nitrophenolate) to 4-aminophenol by sodium borohydride ($NaBH_4$) was adopted (Figure 3A).[20] The 4-nitrophenolate anion formation from 4-nitrophenol upon the addition of borohydride is indicated by the peak shift from 317 nm (due to 4-nitrophenol) to 400 nm (4-nitrophenolate) (Figure S3).[21,22] Such catalytic reaction can be easily monitored via UV−vis spectroscopy from the adsorption decrease of 4-nitrophenolate anion at 400 nm,[23−25] leading to the direct measurement of the catalytic rate constant (k).[26] As shown in Figure 3B, the Au-catalyzed reduction of 4-nitrophenolate anion by BH_4^- is monitored at λ_{max} = 400 nm through spectrophotometry.

In order to quantitatively evaluate the catalytic performance of these catalysts, the rate constant (k) of the catalytic reaction was taken as the parameter to reflect the influence of catalysts on the reaction. In this reaction system, for all experiments, the initial concentrations of 4-nitrophenol and $NaBH_4$ were kept at 1×10^{-4} and 1×10^{-2} M, respectively. Due to the much higher concentration of BH_4^- than that of 4-nitrophenol, the concentration of BH_4^- could be taken as a constant during the whole reaction process. Therefore, the experimental system could be taken as the pseudo-first-order kinetics with respect to 4-nitrophenol (or 4-nitrophenolate).[22] As show in Figure 3B, at room temperature, the regenerated catalyst (Au-R) presented the largest k (0.75×10^{-5} mol/L/min) among the three catalysts (Au-F: 0.51×10^{-5} mol/L/min, Au-R: 0.38×10^{-5} mol/L/min), indicating the highest catalytic activity of Au-R among these catalysts. Moreover, due to its lowest Au loading (Au 0.45 wt % in Au-R), one can see the mass-normalized activity or Au utilization of Au-R is more than 3 times of the Au-F and 5 times of the Au-S.

In order to figure out whether such a highly efficient regeneration method is also applicable for fresh catalysts, we reformed or redispersed the Au nanoparticle on fresh catalyst (Au-F, Au 1.0 wt %) with the same redispersion protocol. The obtained sample was labeled as Au-R_1. Interestingly, as shown in Figure S6, the catalytic activity (0.75×10^{-5} mol/L/min) of catalyst Au-R regenerated from the sintered one (Au-S) is slightly higher than that (0.70×10^{-5} mol/L/min) of the one (Au-R_1) regenerated from fresh (Au-F); more importantly, the activity (0.70×10^{-5} mol/L/min) of the obtained Au-R_1 is much higher than that of the fresh one (Au-F, 0.51×10^{-5} mol/L/min), indicating such a regeneration method is also practically applicable for fresh catalysts. Moreover, we further compared the catalytic activity of the regenerated Au-R (Au 0.45 wt %) with the fresh Au/C (Au 0.50 wt %, labeled as Au-$F_{0.5}$) at about the same Au loading. Interestingly, as shown in Figure S6, the catalytic activity (0.75×10^{-5} mol/L/min) of the regenerated Au-R is higher than that (0.40×10^{-5} mol/L/min) of Au-$F_{0.5}$, indicating higher Au utilization of the regenerated catalyst obtained here probably due to the smaller size of the regenerated Au nanoparticles as shown in Figures 1 and 2.

Activation energy (E_a) in the Arrhenius equation is an empirical parameter for all chemical reactions and reflects the energy needed for a reaction to occur

$$k = Ae^{-E_a/RT}$$

where prefactor A is a constant known as the Arrhenius factor, k is the rate constant of the reaction at temperature T (in Kelvin), and R is the universal gas constant.

On the basis of the reaction rate constant (k) for each catalyst obtained at four different temperatures (298, 303, 308, and 313 K), the apparent activation energy (E_a) was obtained based on the linear fitting of ln k versus $1/T$ with the Arrhenius equation. As shown in Figure 4, the activation energy of regenerated Au/C (Au-R: 27.1 kJ/mol) was lower than that of fresh Au/C (Au-F: 33.6 kJ/mol) and sintering Au/C (Au-S: 41.5 kJ/mol), confirming the highest catalytic activity of Au-R for the reaction between 4-nitrophenol and $NaBH_4$.

Moreover, it has been known that the surface valence state of the nanoparticles is also an important factor in determining the catalytic properties of catalysts. In this case, we did the XPS analysis for these catalysts and compared the valences of the gold before and after the sintering or redispersion process. From Table 1 and Figure S7, one can see that Au^{3+} species disappeared along with the appearance of Au^0 species after sintering. The possible reason is that the Au^{3+} is reduced by carbon at high temperature (900 °C). After the regeneration process, the content of Au^+ species increased a lot. Therefore, the higher activity or Au utilization of Au-R could be attributed in part to the existence of a large amount of Au^+ since it has

DOI: 10.1021/acs.jpcc.7b08787
J. Phys. Chem. C 2017, 121, 25882−25887

been known that the Au^+ species is the main active component for some catalytic processes.[27]

It has been known that the high-index facets were catalytically more active than the low-index facets.[28−30] To further validate such a type of structure−activity relationship in these Au catalysts, the XRD spectra were obtained as shown in Figure 5A. In this case, the intensity ratio between the (200) peak and (111) peak ($I(200)/I(111)$) was adopted to quantify the amount of the Au(200) facet on these catalysts. As expected,[18] it was found that the ratio decreased after sintering while increased hugely after the regeneration process. The positive correlation shown in Figure 5B between the ratio and the catalytic activity indicates unambiguously that the Au (200) facet is more active than the (111) facet for the catalytic reduction of 4-nitrophenolate by $NaBH_4$, different from the observation that the Pt(111) facet is more active than the (200) facet for methanol electrooxidation.[18]

4. CONCLUSION

In summary, with additional inexpensive carbon support to improve the redispersion of Au, the sintered Au/C catalyst was regenerated highly efficiently in catalytic activity for 4-nitrophenolate reduction with Au utilization tripled. In principle, such a simple method can potentially make Au or other precious metals potentially sustainable for their application in industry.

■ ASSOCIATED CONTENT

Supporting Information

The Supporting Information is available free of charge on the ACS Publications website at DOI: 10.1021/acs.jpcc.7b08787.

Materials and methods; experimental details; control experiments (PDF)

■ AUTHOR INFORMATION

Corresponding Author

*E-mail: weilinxu@ciac.ac.cn.

ORCID

Weilin Xu: 0000-0001-7140-8060

Notes

The authors declare no competing financial interest.

■ ACKNOWLEDGMENTS

The work was funded by the National Basic Research Program of China (973 Program, 2014CB932700), the National Natural Science Foundation of China (U1601211, 21503211, 21633008, 21733004, 21721003, 21503212, and 21433003), K. C. Wong Education Fundation and Science and Technology Innovation Foundation of Jilin Province for Talents Cultivation (20160519005JH, L20142200005), and Jilin Youth Foundation (20160520137JH).

■ REFERENCES

(1) Tsukamoto, D.; Shiraishi, Y.; Sugano, Y.; Ichikawa, S.; Tanaka, S.; Hirai, T. Gold Nanoparticles Located at the Interface of Anatase/Rutile TiO_2 Particles as Active Plasmonic Photocatalysts for Aerobic Oxidation. *J. Am. Chem. Soc.* **2012**, *134*, 6309−15.

(2) Carrettin, S.; McMorn, P.; Johnston, P.; Griffin, K.; Hutchings, G. J. Selective Oxidation of Glycerol to Glyceric Acid Using a Gold Catalyst in Aqueous Sodium Hydroxide. *Chem. Commun.* **2002**, 696−697.

(3) Qi, P.; Chen, S.; Chen, J.; Zheng, J.; Zheng, X.; Yuan, Y. Catalysis and Reactivation of Ordered Mesoporous Carbon-Supported Gold Nanoparticles for the Base-Free Oxidation of Glucose to Gluconic Acid. *ACS Catal.* **2015**, *5*, 2659−2670.

(4) Xu, X.; Fu, Q.; Guo, X.; Bao, X. A Highly Active "Nio-on-Au" Surface Architecture for Co Oxidation. *ACS Catal.* **2013**, *3*, 1810−1818.

(5) Saha, S.; Pal, A.; Kundu, S.; Basu, S.; Pal, T. Photochemical Green Synthesis of Calcium-Alginate-Stabilized Ag and Au Nanoparticles and Their Catalytic Application to 4-Nitrophenol Reduction. *Langmuir* **2010**, *26*, 2885−2893.

(6) Kuroda, K.; Ishida, T.; Haruta, M. Reduction of 4-Nitrophenol to 4-Aminophenol over Au Nanoparticles Deposited on Pmma. *J. Mol. Catal. A: Chem.* **2009**, *298*, 7−11.

(7) Sie, S. T. Consequences of Catalyst Deactivation for Process Design and Operation. *Appl. Catal., A* **2001**, *212*, 129−151.

(8) David Jackson, S. Processes Occurring During Deactivation and Regeneration of Metal and Metal Oxide Catalysts. *Chem. Eng. J.* **2006**, *120*, 119−125.

(9) Daley, R. A.; Christou, S. Y.; Efstathiou, A. M.; Anderson, J. A. Influence of Oxychlorination Treatments on the Redox and Oxygen Storage and Release Properties of Thermally Aged Pd-Rh/$Ce_xZr_1-XO_2/Al_2O_3$ Model Three-Way Catalysts. *Appl. Catal., B* **2005**, *60*, 117−127.

(10) Galisteo, F. C.; Mariscal, R.; Granados, M. L.; Fierro, J. L. G.; Daley, R. A.; Anderson, J. A. Reactivation of Sintered Pt/Al_2O_3 Oxidation Catalysts. *Appl. Catal., B* **2005**, *59*, 227−233.

(11) Hatanaka, M.; Takahashi, N.; Tanabe, T.; Nagai, Y.; Dohmae, K.; Aoki, Y.; Yoshida, T.; Shinjoh, H. Ideal Pt Loading for a Pt/CeO_2-Based Catalyst Stabilized by a Pt−O−Ce Bond. *Appl. Catal., B* **2010**, *99*, 336−342.

(12) Le Normand, F.; Borgna, A.; Garetto, T. F.; Apesteguia, C. R.; Moraweck, B. Redispersion of Sintered Pt/Al_2O_3 Naphtha Reforming Catalysts: An in Situ Study Monitored by X-Ray Absorption Spectroscopy. *J. Phys. Chem.* **1996**, *100*, 9068−9076.

(13) Morgan, K.; Goguet, A.; Hardacre, C. Metal Redispersion Strategies for Recycling of Supported Metal Catalysts: A Perspective. *ACS Catal.* **2015**, *5*, 3430−3445.

(14) Duan, X.; Tian, X.; Ke, J.; Yin, Y.; Zheng, J.; Chen, J.; Cao, Z.; Xie, Z.; Yuan, Y. Size Controllable Redispersion of Sintered Au Nanoparticles by Using Iodohydrocarbon and Its Implications. *Chem. Sci.* **2016**, *7*, 3181−3187.

(15) Duan, X.; Yin, Y.; Tian, X.; Ke, J.; Wen, Z.; Zheng, J.; Hu, M.; Ye, L.; Yuan, Y. C−X (X = Cl, Br, I) Bond Dissociation Energy as a Descriptor for the Redispersion of Sintered Au/Ac Catalysts. *Chin. J.Catal.* **2016**, *37*, 1794−1803.

(16) Sa, J.; Goguet, A.; Taylor, S. F.; Tiruvalam, R.; Kiely, C. J.; Nachtegaal, M.; Hutchings, G. J.; Hardacre, C. Influence of Methyl Halide Treatment on Gold Nanoparticles Supported on Activated Carbon. *Angew. Chem., Int. Ed.* **2011**, *50*, 8912−6.

(17) Sá, J.; Taylor, S. F. R.; Daly, H.; Goguet, A.; Tiruvalam, R.; He, Q.; Kiely, C. J.; Hutchings, G. J.; Hardacre, C. Redispersion of Gold Supported on Oxides. *ACS Catal.* **2012**, *2*, 552−560.

(18) Ruan, M.; Sun, X.; Zhang, Y.; Xu, W. Regeneration and Enhanced Catalytic Activity of Pt/C Electrocatalysts. *ACS Catal.* **2015**, *5*, 233−240.

(19) Ruan, M.; Jiao, M.; Song, P.; Wu, Z.; Wang, Y.; Wu, Z.; Xu, W.; Wang, Y. Morphology-Tuning-Induced Highly Efficient Regeneration of Pt/C Nanoelectrocatalysts. *J. Phys. Chem. C* **2017**, *121*, 3911−3919.

(20) Pradhan, N.; Pal, A.; Pal, T. Silver Nanoparticle Catalyzed Reduction of Aromatic Nitro Compounds. *Colloids Surf., A* **2002**, *196*, 247−257.

(21) Praharaj, S.; Nath, S.; Ghosh, S. K.; Kundu, S.; Pal, T. Immobilization and Recovery of Au Nanoparticles from Anion Exchange Resin: Resin-Bound Nanoparticle Matrix as a Catalyst for the Reduction of 4-Nitrophenol. *Langmuir* **2004**, *20*, 9889−9892.

(22) Hayakawa, K.; Yoshimura, T.; Esumi, K. Preparation of Gold-Dendrimer Nanocomposites by Laser Irradiation and Their Catalytic Reduction of 4-Nitrophenol. *Langmuir* **2003**, *19*, 5517−5521.

(23) Herves, P.; Pérez-Lorenzo, M.; Liz-Marzán, L. M.; Dzubiella, J.; Lu, Y.; Ballauff, M. Catalysis by Metallic Nanoparticles in Aqueous Solution: Model Reactions. *Chem. Soc. Rev.* **2012**, *41*, 5577−5587.
(24) Esumi, K.; Isono, R.; Yoshimura, T. Preparation of Pamam-and Ppi-Metal (Silver, Platinum, and Palladium) Nanocomposites and Their Catalytic Activities for Reduction of 4-Nitrophenol. *Langmuir* **2004**, *20*, 237−243.
(25) Fenger, R.; Fertitta, E.; Kirmse, H.; Thünemann, A.; Rademann, K. Size Dependent Catalysis with Ctab-Stabilized Gold Nanoparticles. *Phys. Chem. Chem. Phys.* **2012**, *14*, 9343−9349.
(26) Ghosh, S. K.; Mandal, M.; Kundu, S.; Nath, S.; Pal, T. Bimetallic Pt−Ni Nanoparticles Can Catalyze Reduction of Aromatic Nitro Compounds by Sodium Borohydride in Aqueous Solution. *Appl. Catal., A* **2004**, *268*, 61−66.
(27) Malta, G.; Kondrat, S. A.; Freakley, S. J.; Davies, C. J.; Lu, L.; Dawson, S.; Thetford, A.; Gibson, E. K.; Morgan, D. J.; Jones, W.; et al. Identification of Single-Site Gold Catalysis in Acetylene Hydrochlorination. *Science* **2017**, *355*, 1399−1403.
(28) Zhang, Q.; Wang, H. Facet-Dependent Catalytic Activities of Au Nanoparticles Enclosed by High-Index Facets. *ACS Catal.* **2014**, *4*, 4027−4033.
(29) Seo, B.; Choi, S.; Kim, J. Simple Electrochemical Deposition of Au Nanoplates from Au(I) Cyanide Complexes and Their Electrocatalytic Activities. *ACS Appl. Mater. Interfaces* **2011**, *3*, 441−446.
(30) Hebié, S.; Cornu, L.; Napporn, T. W.; Rousseau, J.; Kokoh, B. K. Insight on the Surface Structure Effect of Free Gold Nanorods on Glucose Electrooxidation. *J. Phys. Chem. C* **2013**, *117*, 9872−9880.

DOI: 10.1021/acs.jpcc.7b08787
J. Phys. Chem. C 2017, 121, 25882−25887